BIOCHEMISTRY
including biophysical chemistry & molecular biology
Article

Biochemistry **2010,** *49,* 3525–3533 3525
DOI: 10.1021/bi901279e

Effects of the Nature and Concentration of Salt on the Interaction of the HIV-1 Nucleocapsid Protein with SL3 RNA†

Shreyas S. Athavale,‡ Wei Ouyang, Mark P. McPike, Bruce S. Hudson, and Philip N. Borer*

Department of Chemistry, Syracuse University, Syracuse, New York 13244 ‡*Current address: Department of Chemistry and Biochemistry, Georgia Institute of Technology, Atlanta, GA 30332.*

Received July 25, 2009; Revised Manuscript Received March 25, 2010

ABSTRACT: The mature nucleocapsid protein of HIV-1, NCp7, and the NC domains in gag precursors are attractive targets for anti-AIDS drug discovery. The stability of the 1:1 complex of NCp7 with a 20mer mimic of stem−loop 3 RNA (SL3, also called ψ-RNA, in the packaging domain of genomic RNA) is strongly affected by changes in ionic strength. NC domains recognize and specifically package genomic HIV-1 RNA, while electrostatic attractions and high concentrations of protein and RNA drive NCp7 to completely coat the RNA in the mature virion. The specific interactions of NCp7 binding to loop bases of SL3 produce 1:1 complexes in solutions that have a NaCl concentration of ≥0.2 M, while the electrostatic interactions can dominate at ≤0.15 M NaCl, leading to complexes that have a mainly 1:2 RNA:protein ratio. Persistent, nonequilibrium mixtures of 1:1 and protein-excess complexes can exist at these lower salt concentrations, where the distribution of complexes depends on the order of addition of RNA and protein. Adding salt causes rapid rearrangement of metastable multiprotein complexes to a 1:1 ratio. The stability of complexes is also affected by the nature of the added salt, with 0.018 M $MgCl_2$ and added 0.200 M NaCl producing the same K_d (21 ± 2 nM); acetate ion stabilizes the 1:1 complex by a factor of more than 2 compared to the same concentration of chloride ion. Maintaining a salt concentration of 0.2 M NaCl or 18 mM $MgCl_2$ is sufficient for experiments to distinguish drug candidates that disrupt the specific SL3−NCp7 interactions in the 1:1 complex.

The nucleocapsid protein of HIV-1 is an attractive anti-AIDS drug target. In addition to its role in packaging the RNA (*1*−*4*), it has chaperoning functions (*5*, *6*), helps refold the RNA dimer (*7*−*9*), and anneals the primer tRNA onto genomic RNA for reverse transcription (*10*, *11*). It also interacts with viral proteins, including reverse transcriptase (*12*, *13*), and the accessory protein, Vpr, to play a role in stable integration of the proviral DNA in the chromosomes of infected cells (*14*). Drugs targeted at NC have the potential to interfere with critical functions at many stages of the viral infection cycle (*6*, *9*, *11*, *15*−*18*).

In retroviruses similar to HIV-1, ~2000 polyprotein precursors (gag and gag-pol) assemble at the inner membrane of the forming virion (*19*−*21*). Each of these proteins contains a nucleocapsid domain that is required for packaging genomic RNA into new virus particles. The 55 kDa gag precursor polyprotein is later processed by the viral protease to structural proteins, including the mature NCp7[1] (*20*). NC domains within gag precursors bind to the RNA, with several RNA−NC interactions responsible for full discrimination of genomic from nongenomic RNA (*22*−*27*). Both sequence-specific and non-sequence-specific contacts contribute to the free energy of binding (*22*−*30*).

The NC domain of gag precursor proteins and the mature NCp7 protein bind with high affinity to stem−loop 3 (SL3, also called the packaging or Ψ-loop) located at nucleotides 312−325 in the 5′-untranslated region of genomic RNA (see Figure 1). Sequence-specific interactions are important in defining the structure of the SL3−NCp7 packaging complex (*31*). G318 stacks on W37, leading to nearly full quenching of the tryptophan fluorescence and straightforward analysis of binding isotherms (*27*, *31*−*35*). The dissociation constant was reported to be 28 ± 6 nM in 0.2 M NaCl for the complex (*32*), revised here to 21 ± 2 nM. Non-sequence-specific interactions, which are largely electrostatic, also contribute to affinity because of the high charges of the fully ionized species: −19 for the SL3 20mer and +9 for NCp7 (pNL4-3 strain; see the legend of Figure 1).

The non-sequence-specific interaction dominates in the mature virion where there is roughly one NCp7 per 7−10 nucleotides. This interaction allows the RNA and protein to collapse to a chromatin-like density. The protein concentration is >10 mM in the mature nucleocapsid, so more than 95% of RNA 10mer segments would be bound by NCp7 even for sequences with a 1000-fold lower affinity than SL3.

It has been appreciated for more than 10 years that complexes of ~20mer oligonucleotides with NCp7 can have RNA:protein stoichiometries other than 1:1 (*27*, *32*, *36*−*42*). Our lab noted unusual effects in the reproducibility of SL3−NCp7 binding assays at ≤0.15 M NaCl; we suggested that this was due to the presence of competing complexes with protein in excess (*27*).

†Supported in part by National Institutes of Health Grant R01 GM32691.

*To whom correspondence should be addressed. Phone: (315) 443-5925. Fax: (315) 443-4070. E-mail: pnborer@syr.edu.

[1]Abbreviations: SL3, stem−loop 3 with unpaired residues at G317, G318, A319, and G320 of the 5′-leader of HIV-1 genomic RNA; NCp7, HIV-1 nucleocapsid protein; K_d, equilibrium constant for the dissociation of a bimolecular complex; P_t, total concentration of protein; R_t, total strand concentration of RNA; MS, mass spectrometry; ESI, electrospray ionization; SPR, surface plasmon resonance; ITC, isothermal titration calorimetry.

Published on Web 04/02/2010

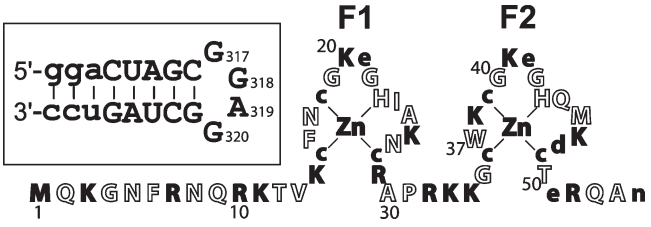

FIGURE 1: Mature NCp7 protein from the pNL4-3 strain (wild-type I1 has been replaced with M1 for efficient expression in *Escherichia coli*). Residues carrying a charge are shown as filled letters (uppercase for positive and lowercase for negative); at neutral pH, NCp7 from pNL4-3 carries a +9 net charge [+1 (N-terminus), +15 (R, K side chains), −4 (D, E side chains), +4 (Zn^{2+}), −6 (cysteine thiolates), −1 (C-terminus)]. The inset shows the SL3 sequence; lowercase residues are not present in wild-type SL3.

This work was motivated by the need to distinguish conditions that cause the occurrence of R_1P_1 or $R_1P_{\geq 2}$ complexes, particularly as influenced by the nature and concentration of counterions, and to resolve disagreements in the literature regarding K_d values of the 1:1 complex. In addition, we provide a firm basis for characterizing the properties of R_1P_1 complexes that provide the specificity of packaging genomic RNA.

We show that metastable, nonequilibrium mixtures of protein-excess complexes can be rearranged to specific R_1P_1 complexes with an increase in ionic strength and that the persistence of metastable complexes can be influenced by the order of addition of RNA and protein at low ionic strengths. Also, the metastable complexes can be eliminated by replacement of Na^+ as the RNA counterion with Mg^{2+}; 0.018 M Mg^{2+} added to the buffer used here produces the same K_d as added 0.200 M Na^+. Other counterions are also explored. Lack of attention to these and other experimental details is shown to be a major source of disagreement among published K_d values.

EXPERIMENTAL PROCEDURES

NCp7 Preparation. The 55-amino acid NCp7 was prepared, and the concentrations were estimated as described previously (*27*, *32*). Protein stocks at 300−1000 μM were stored for several months without degradation in a 25 mM acetate buffer (pH 5) with 10% glycerol, 10 mM dithiothreitol, 0.05 mM EDTA, 25 mM NaCl, and 0.1 mM $ZnCl_2$ at −80 °C. "AddNA" assays with SL3 added to 0.3 μM NCp7 were repeated as a positive control each day before any other experiment was performed (*27*, *32*). NCp7 preparations were rejected if they failed to exhibit at least 95% quenching with a 3-fold excess of the 20mer, SL3-GGUG, GGACUAGCGGUGGCUAGUCC, which has a K_d of 10 nM (*32*).

SL3 RNA. SL3 was purchased from IDT DNA Technologies (Coralville, IA) and used without further purification. The RNA was heated to 95 °C for 3 min, cooled on ice, and stored on ice prior to use.

Fluorescence Buffer. The buffer for the fluorescence assays contained 5.0 mM sodium phosphate ($Na_{1.38}H_{1.62}PO_4$; 5.0 mM NaH_2PO_4 was adjusted to pH 7.0 with NaOH), 0.10 mM $ZnCl_2$, 0.01% poly(ethylene glycol), and one of the added salts: NaCl, KCl, $NaC_2H_3O_2$, $MgCl_2$, Na_2SO_4, or $MgSO_4$ (at concentrations specified in Figures 2−6). The ionic strength of each buffer is the contribution from the added salt plus 0.0091 M for sodium phosphate and $ZnCl_2$; ionic strength contributions are beyond the fourth decimal place for SL3 RNA and NCp7 at submicromolar concentrations. In this paper, the buffer with added 0.200 M NaCl is termed the μ = 0.209 M buffer, or by specifying only the nature and concentration of the added salt.

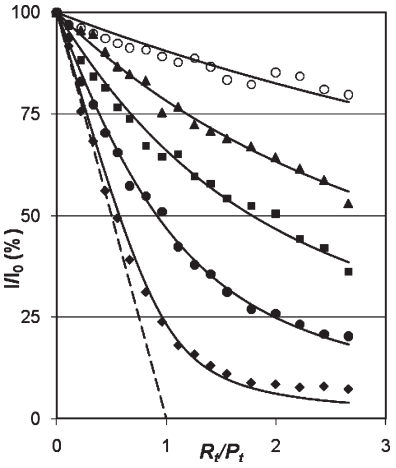

FIGURE 2: Experimental AddNA assays in which SL3 was added to NCp7. The binding isotherms are at progressively higher salt concentrations, from bottom to top, with the long-dash limit line representing infinitely high affinity for an R_1P_1 complex ($K_d \rightarrow 0$): (◆) 0.200 M NaCl (fitted with K_d = 21 nM), (●) 0.300 M (K_d = 120 nM), (■) 0.400 M (K_d = 380 nM), (▲) 0.500 M (K_d = 840 nM), and (○) 0.800 M (K_d = 2600 nM). The total protein concentration (P_t) is 0.30 μM.

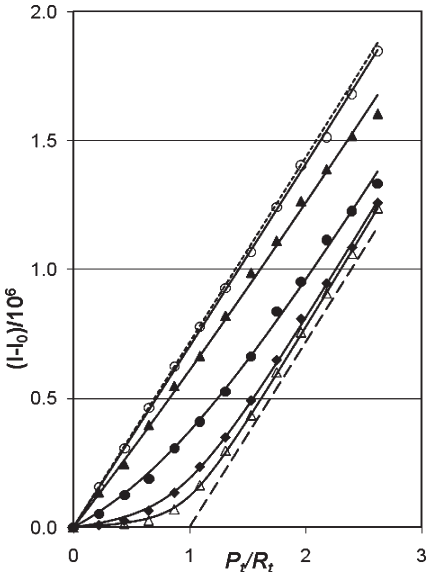

FIGURE 3: Experimental AddPro assays in which NCp7 was added to SL3 (total RNA concentration, R_t, of 0.30 μM). As in Figure 2, isotherms at low salt concentrations appear near the bottom of the plot. $I - I_0$ is the difference between the measured fluorescence and the fluorescence without protein. The symbols are defined in the legend of Figure 2, with the addition of 0.150 M NaCl (△). Solid lines show isotherms fitted using a K_d of 9 nM for 0.150 M NaCl, a K_d of 25 nM for 0.200 M NaCl, a K_d of 140 nM for 0.300 M NaCl, and a K_d of 1120 nM for 0.500 M, 5,300 nM, for 0.800 M NaCl. The limit lines represent $K_d \rightarrow 0$ (long dashes) and $K_d^{-1} \rightarrow 0$ (short dashes) for an R_1P_1 complex.

AddNA Assay. Ideal AddNA assays for 1:1 complexes are shown in Figure S1 of the Supporting Information to illustrate the expected response for a variety of K_d values. Assays were performed by adding SL3 RNA (50 μM stock) in aliquots of 1.5−3 μL to 0.30 μM NCp7 in 2.00 mL of the fluorescence buffer in a 10 mm × 10 mm path length quartz fluorescence cuvette (NSG Precision Cells) along with an 8 mm × 1.5 mm stir bar.

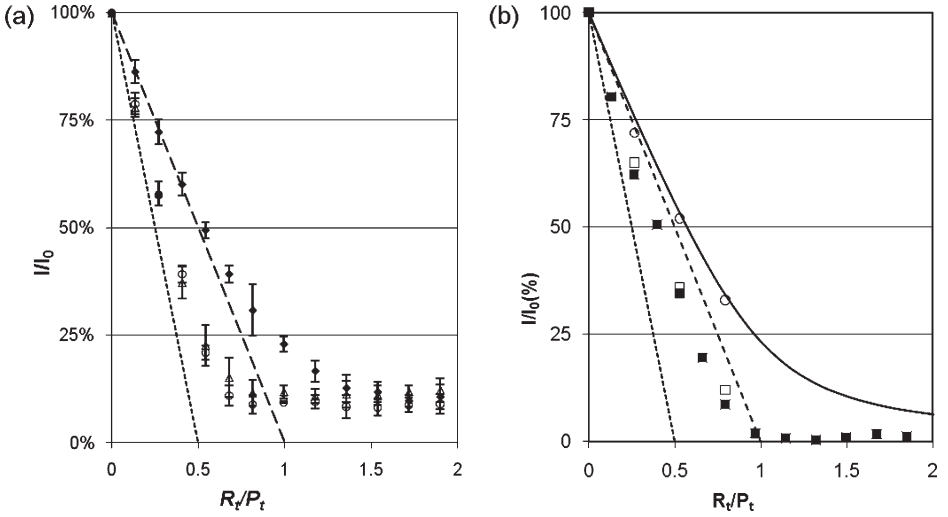

FIGURE 4: AddNA assays at low NaCl concentrations measured as described in the legend of Figure 2. The limit lines are for R_1P_1 (long dashes) and R_1P_2 (short dashes; this line intersects the x-axis at an R_t/P_t mole ratio of 1/2). (a) Solid diamonds show 0.200 M NaCl data; the error bars indicate one standard deviation about the average of three replicates: (△) 0.150 and (○) 0.100 M NaCl. (b) Filled squares show data for a full titration at 0.050 M NaCl. Empty squares show the end points of three titrations with the identical spacing of the earlier points. At each end point, the NaCl concentration was increased to 0.200 M and the fluorescence increased to the values indicated by empty circles, which fall near the solid line calculated for a K_d of 21 nM.

The fluorescence of the free NCp7 (i.e., the fraction of the protein not bound to SL3) was measured using a PTI QM-4/2003SE fluorometer at 349.9 nm emission using 290 nm excitation, a 4 nm excitation band-pass, and a 1.5−3 nm emission band-pass. The fluorescence titration curves obtained were fitted to a model assuming 1:1 stoichiometry for the ratio of NCp7 bound to SL3.

The titration curves were fitted to eq 1 as previously reported (*32*).

$$(I - I_\infty)/I_0 = \{-(R_t - P_t + K_d) + [(R_t - P_t + K_d)^2 + 4P_tK_d]^{1/2}\}/2P_t + I_\infty \quad (1)$$

where P_t and R_t are the total protein and total SL3 concentrations, respectively, I is the measured fluorescence intensity, I_0 is the intensity when $R_t = 0$, I_∞ is the intensity at saturation, and K_d is the dissociation constant. The equation was derived by using standard assumptions that $I - I_\infty$ is directly proportional to the free protein concentration, P_f, that $P_t = P_f + P_{bound}$, $R_t = R_f + R_{bound}$, and $K_d = (R_fP_f)/(RP)$. The data were fitted using OriginPro version 7.5; P_t was fixed at 0.30 μM and I_∞ at zero, and K_d was the only adjustable parameter. It was determined that there was no improvement in the fit when I_∞ was allowed to be an adjustable parameter. This is consistent with the >95% quenching standard for SL3-GGUG, described in NCp7 Preparation.

AddPro Assay. Ideal AddPro assays for 1:1 complexes at a constant R_t of 0.3 μM are illustrated in Figure S2 of the Supporting Information. Assays were performed by adding NCp7 (50 μM stock) in aliquots of 1.5−3 μL to 0.30 μM SL3 in 2.00 mL of the fluorescence buffer (added 0.010−0.800 M NaCl), and fluorescence was measured as described for the AddNA assays. At NaCl concentrations lower than 0.15 M, the starting concentrations of SL3 and NCp7 were diluted 4-fold to move the titration curves away from the 1:1 line.

Fitting details are similar to the AddNA titrations, except the data were fitted to eq 2.

$$I - I_0 = m\{P_t - R_t - K_d + [(R_t + P_t + K_d)^2 - 4R_tP_t]^{1/2}\}/2 \quad (2)$$

The parameters are the same as in eq 1, except that m is the slope of plots for cases in which no interaction occurs or when no RNA is present, and I_0 is the blank intensity. The data were fitted using OriginPro version 7.5 with R_t fixed at the starting value (0.30 or 0.075 μM), and K_d and m as the adjustable parameters. Fitting was less reproducible if m was not an adjustable parameter.

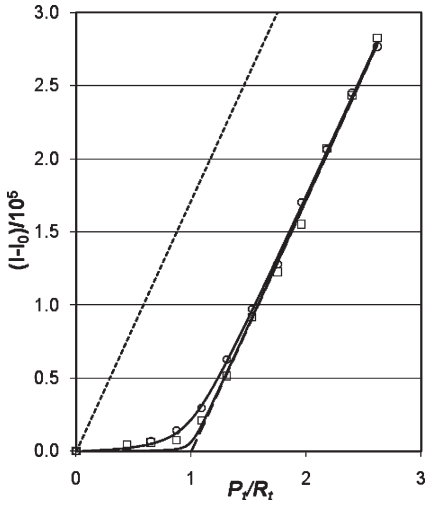

FIGURE 5: AddPro assays for 0.100 and 0.050 M NaCl at a total RNA concentration, R_t, of 0.075 μM. Solid lines show isotherms fitted to the data: (○) 0.100 M NaCl (K_d = 1.4 nM) and (□) 0.050 M NaCl (K_d = 0.3 nM). Limit lines are as in Figure 3. The starting NCp7 and SL3 concentrations were diluted 4-fold from those shown in Figure 3. Without this dilution, titrations for 0.100 and 0.050 M NaCl proceed along the x-axis to the breakpoint at P_t/R_t = 1 and then follow the 1:1 line (data not shown).

Alternative Counterions. AddNA assays were performed to assess the effect of K^+, Mg^{2+}, OAc^- (acetate), and SO_4^{2-} ions on the binding equilibria. Reagent grade crystals of NaCl, KCl, $MgCl_2$, Na_2SO_4, and $MgSO_4$ were used. Standardized solutions of NaOH were mixed with a standardized acetic acid solution to achieve accurate concentrations of NaOAc as the salt is strongly deliquescent (1.000 M solutions of NaOH and HOAc were purchased from Sigma-Aldrich and 2.000 M solutions from Ricca Chemical Co.).

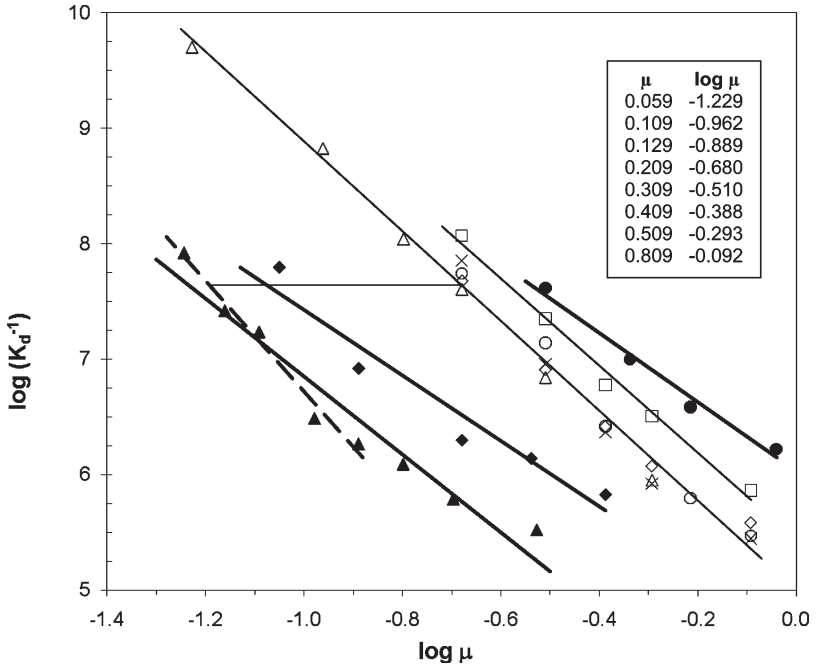

FIGURE 6: Dependence of NCp7−SL3 binding on ionic strength for six salts. Empty symbols and thin lines are for salts with monovalent ions: sodium chloride (AddPro) (△), sodium chloride (AddNA, this work) (◇), sodium chloride [AddNA, previously reported (*27*)] (○), potassium chloride (AddNA, this work) (×), and sodium acetate (AddNA) (□). Data for salts containing divalent ions are shown with filled symbols and thick lines: magnesium chloride (AddNA) (▲) (the shorter dashed line was fitted to points with $\mu \leq 0.129$ M), magnesium sulfate (AddNA) (◆), and sodium sulfate (Add NA) (●). Best-fit lines for the monovalent ions had the following slopes and standard errors: NaCl, -3.84 ± 0.15; KCl, -4.16 ± 0.42 (line not shown); NaOAc, -3.77 ± 0.22. The thin horizontal line links the $MgCl_2$ and NaCl lines where both have K_d values of 23 nM (at 0.20 M NaCl and 0.018 M $MgCl_2$). The nomogram (top right) helps to interpret the *x*-axis. It includes several μ values used in the experiments and their corresponding logarithms [μ includes the 0.009 M contribution from the invariant buffer components (sodium phosphate and zinc chloride)].

RESULTS

Validation of AddPro Assays. Prior to the use of AddPro assays, their usefulness should be validated with respect to traditional AddNA titrations. Figures 2 and 3 compare AddNA and AddPro under conditions where the AddNA data signify the formation of a 1:1 complex between SL3 RNA and NCp7 (*27*, *32*). In both figures, the points that lie nearest the long-dash 1:1 line are for complexes that have the highest affinity (lowest salt concentration), with isotherms rising progressively higher as the salt concentration increases [the long-dash line denotes a complex for which the binding constant ($1/K_d$) approaches infinity]. In the AddNA assays, the total RNA concentration, R_t, increases from left to right along the horizontal axis; R_t/P_t is the mole ratio of total RNA over total protein, and the P_t of 0.30 μM is held constant. AddPro assays have P_t, increasing from left to right, a constant R_t of 0.30 μM, and again a varying NaCl concentration. As the salt concentration increases above 0.2 M, the affinity decreases as expected for the association of the highly charged protein and RNA. The legends of Figures 2 and 3 give the best-fit K_d values for these particular data sets; the agreement between the two assays is excellent at 0.2 and 0.3 M NaCl, but the K_d values agree less well at higher salt levels. As one can see from Figure 3, AddPro assays exhibit very little difference between the data points at ≥0.5 M NaCl and the "no binding" limit line (short dashes). Near this limit the fitting is very sensitive to small deviations in the experimental data. Thus, AddPro K_d values at high salt concentrations are less reproducible than for NaCl concentrations near 0.2 M. It is also true that the fits for AddNA titrations at high salt concentrations are less reliable than those near 0.2 M salt as the fluorescence intensities at the right end of the binding isotherms measured at high salt concentrations do not approach the limit, I_∞, characteristic of an RNA-saturated 1:1 complex. The general result is that the AddPro assays give the same K_d values as AddNA assays within experimental error. Importantly, the order of addition of RNA and protein is irrelevant in the physiological range of salt concentration, consistent with a 1:1 complex in rapid equilibrium with free RNA and protein.

Order of Addition of RNA and Protein at Low Salt Concentrations. The issues that occur at lower ionic strengths in AddNA assays are illustrated in Figure 4. The data measured at 0.100 and 0.150 M NaCl (Figure 4a) fall between the lines for complexes with stoichiometries of 1:1 (long dashes) and 1:2 (short dashes). This indicates that a persistent complex with an excess of protein over RNA ($R_1P_{n>1}$) occurs in addition to R_1P_1 when RNA is added to protein at low salt concentrations. [As a reference, the upper data set (◆) shows the average of three replicate trials in added 0.200 M NaCl in the fluorescence buffer. These points all lie above the thick-dash line, as expected for 1:1 complexes, and the error bars are small.] Data at 0.050 M NaCl (Figure S3 of the Supporting Information) also fall between the 1:1 and 1:2 lines but are not even reproducible from one day to the next. Adding a 2.00 M NaCl solution to make the final NaCl concentration 0.200 M moves any of the data points below the 1:1 line to the 0.200 M titration curve at the corresponding R_t/P_t ratio (see Figure 4b); this change occurs within the few seconds required for addition and mixing.

By contrast, the AddPro assays for 0.150 M NaCl [Figure 3(△)] and for 0.100 and 0.050 M NaCl (Figure 5) all fall near the 1:1 line, but above it, consistent with 1:1 complexes having high affinity. Thus, when protein is added to RNA, $R_1P_{n>1}$ complexes do not form in this range of salt concentrations, and equilibration

Table 1: K_d Values[a] with Varying NaCl Concentrations

[NaCl] (M)	N	K_d(av) (nM)	K_d(slope) (nM)
0.800	2	3800	4400
0.500	2	980	730
0.400	2	380	310
0.300	3	110 ± 40	110
0.200	38	21 ± 2	23
0.100	5	1.5 ± 0.6	1.9
0.050	2	0.2	0.18
0.010	–	–	0.022

[a]Dissociation constants, K_d(av), are averages of values of individual determinations at the indicated NaCl concentration for the NCp7−SL3 complex (standard deviations are shown for determinations with at least three replicates). The number of replicates is N; K_d(slope) was predicted from the plot in Figure 6. Trailing zeroes in K_d values are not significant digits. K_d values at <0.200 M NaCl are from AddPro assays, whereas values at >0.300 M NaCl are from AddNA data. K_d values averaged in Table 1 for 0.100 and 0.050 M NaCl are from AddPro measurements at an R_t of 0.075 μM. In addition to the indicated NaCl concentration, the buffer components add 0.0091 M to the ionic strength (see Experimental Procedures).

is rapid. At very low salt concentrations (0.010 and 0.025 M NaCl), AddPro titrations also produce mixed R_1P_1 and $R_1P_{n>1}$ complexes (Figure S4 of the Supporting Information). Thus, the range of salt concentrations in which persistent $R_1P_{n>1}$ complexes can occur is <0.200 M NaCl, at least in the submicromolar range of R_t and P_t employed in this work. The fact that persistent $R_1P_{n>1}$ complexes occur only in the AddNA titrations when the NaCl concentration is between 0.050 and 0.15 M is diagnostic of a nonequilibrium situation in which RNA is added to protein. This, and the persistence of nonequilibrium mixtures of $R_1P_{n>1}$ and R_1P_1 complexes at even lower salt concentrations, calls into doubt many previous determinations of affinity assumed to be for R_1P_1 complexes (see Discussion).

Averages of replicate determinations of K_d for the 1:1 complex are reported in the first three columns of Table 1 at several concentrations of NaCl. K_d values at <0.200 M NaCl are from AddPro assays, whereas values at >0.300 M NaCl are from AddNA data. K_d values averaged in Table 1 for 0.100 and 0.050 M NaCl are from AddPro measurements at an R_t of 0.075 μM.

Global Variation in Ionic Strength. The entire set of data used for determinations of K_d values in NaCl, KCl, NaOAc, $MgCl_2$, Na_2SO_4, and $MgSO_4$ is encompassed in Figure 6. Individual titrations for the latter five salts are not shown, but K_d values were calculated exclusively from AddNA assays. The highest affinities of NCp7 for SL3 are at the top of the y-axis, and the highest salt concentrations are at the right of the x-axis. Contributions to the ionic strength for the salts used in this work are

$$\mu_{salt} = 0.5([C]Z_C^2 + [A]Z_A^2) \quad (3)$$

where C is the cation and A is the anion of the salt in question and Z_C and Z_A are the charges on the respective ions. For the singly charged ions in NaCl, KCl, and NaOAc, μ_{salt} equals the molar concentration. The total ionic strength, μ, is the sum of μ_{salt} plus 0.009 M, which is the contribution of the buffer components to the ionic strength. Slopes of the best fit lines for the monovalent salts are given in the legend of Figure 6.

The AddPro assays in NaCl give access to binding constants, K_d^{-1}, that are nearly 2 orders of magnitude higher than those that can be surveyed using AddNA assays (data points at the top of Figure 6). The whole collection of data points in NaCl includes those measured in this work by AddPro (△) and AddNA (◇) assays, and previously (*27*) by AddNA assays (○). The slopes of the best-fit lines provide a different sort of average from replicate measurements, now over all of the data for a given salt. There is good agreement between these two averages, reflecting the high quality of the measurements. The slopes can be used to predict the K_d at any salt concentration. The predictions for NaCl are compared with the replicate averaged K_d values in the last column of Table 1. These averages compare reasonably well, especially at intermediate salt concentrations. A K_d prediction of 22 pM for 0.010 M NaCl is also included in the table. However, attempts to measure this value failed as the titrations from day to day could not be reproduced in a manner reminiscent of the AddNA assays at low salt concentrations (see Figures S3 and S4 of the Supporting Information).

Nature of the Salt. Plots of K_d as a function of ionic strength for the other salts are also shown in Figure 6. The data for KCl (×) are found among the data points for NaCl, showing that no large change in the affinity of the complex occurred upon substitution of K^+ for Na^+. However, substituting acetate ion (□) for chloride resulted in a substantial displacement from the NaCl line. As the two best-fit lines have nearly the same slope, it can be seen that the complex in OAc^- has approximately half the K_d that it has in Cl^-; i.e., acetate makes the complex approximately twice as stable at the same ionic strength (2.3 times more stable at $\mu = 0.209$ M).

Substituting doubly charged ions for either Na^+ or Cl^- produces a substantial displacement of the best-fit lines in Figure 6. Sulfate stabilizes the complex (●) even more than OAc^-, whereas replacing sodium with magnesium at the same ionic strength strongly destabilizes the complex (▲). $MgSO_4$ shows intermediate behavior (◆), with the destabilizing effect of Mg^{2+} dominating the stabilizing effect of SO_4^{2-}. All of these data sets exhibit curvature about the best-fit straight lines. This is expected as deviations from ideal solutions are more severe for multiply charged ions, especially at higher ionic strengths. The dashed line in Figure 6 was fitted to the $MgCl_2$ data for ionic strengths of ≤ 0.129 M (added 40 mM $MgCl_2$). A thin horizontal line connects the dashed line to the best-fit line for NaCl at added 0.200 M NaCl. This equivalence in K_d occurs at added 18 ± 3 mM $MgCl_2$ ($\mu = 0.063$ M including the buffer salts).

DISCUSSION

The stoichiometry and affinity of NCp7−SL3 complexes depend on the relative contributions of specific binding to the loop bases in SL3 RNA and ionic interactions that are not sequence-specific. The ionic contribution is most profoundly affected by the concentration and nature of added salts. Below 0.200 M NaCl, the order of addition of RNA and protein can lead to the formation of persistent, nonequilibrium (metastable) mixtures of $R_1P_{n>1}$ and R_1P_1 complexes. Variation in the RNA or protein sequence, especially mutations that decrease the stability of the 1:1 complex, plays a role in the distribution of complexes, as well (*43*). A better understanding of these effects, discussed in the next several paragraphs, explains much of the disagreement in reported K_d values for SL3−NCp7 interaction (*22*, *27*, *31*, *32*, *36*−*38*, *41*, *42*, *44*, *45*).

Effect of NaCl Concentration. It is well-known that high salt concentrations suppress ionic interactions. Because of the high charges on fully ionized SL3 (−19) and NCp7 (+9) (see the legend of Figure 1), ionic effects will contribute substantially to the stability of both specific R_1P_1 and nonspecific $R_1P_{n>1}$

complexes. The latter should be most dependent on salt concentration as more ionic interactions are neutralized in the complex. The charge on SL3 RNA is reduced by counterion condensation, and the charges on both RNA and protein are screened by their respective counterion atmospheres. Condensation of sodium ions on SL3 in NaCl should reduce the net charge to −5 to −6 (*46*) (the range arises from assumptions regarding the loop phosphates). Of course, many counterions are released when a complex forms. For instance, six salt bridge interactions were seen between SL3 phosphates and basic side chains of NCp7 in the NMR structure (*31*). Other phosphates are buried in the electropositive binding surface of the protein, as well. Thus, the R_1P_1 complex is likely to retain a substantial net negative charge. A fully ionized R_1P_2 complex would have a charge of −1, which is very near electrical neutrality. Such a complex is likely to have low solubility and is a likely contributor to metastable mixtures. These concepts are borne out by the experiments summarized in Results.

Data presented in Figures 2 and 3 show that at ≥0.2 M NaCl the specific R_1P_1 complex is formed. However, nonspecific binding ($R_1P_{n>1}$ complexes) becomes significant in AddNA assays monitored by fluorescence at ≤0.15 M NaCl (see Figure 4 and Figure S3 of the Supporting Information) and AddPro assays at <0.05 M NaCl (see Figure S4 of the Supporting Information). Early points in AddNA titrations have very little RNA and a large excess of protein. This would favor the production of sparingly soluble $R_1P_{n>1}$ complexes that may rearrange slowly upon further addition of RNA. Of course, a low salt concentration also favors unfolding of the RNA hairpin, and primarily electrostatic interaction with two or more proteins at non-sequence-specific binding sites. The appearance of $R_1P_{n>1}$ complexes at <0.05 M NaCl in AddPro titrations could be due to the high concentration of protein in the microliter droplets that are added to the RNA solution; $R_1P_{n>1}$ complexes could form near the surface of droplets and rearrange only slowly thereafter.

As expected, the electrostatic attraction between RNA and protein produces a large increase in the affinity of the specific 1:1 complex with a decrease in salt concentration. The binding constant, $1/K_d$, changes by $\sim 10^4$ per factor of 10 difference in salt concentration for NaCl, KCl, and NaOAc (see Table 1 and Figure 6).

A consequence of using SL3 in AddNA assays as a daily positive control is that a large number of replicates was available to reduce the standard deviation on the average K_d of 21 ± 2 nM (N = 38). The new average value is somewhat lower than that reported earlier, 28 ± 6 nM (*32*), which was obtained from fewer determinations and using the solver function in Microsoft Excel. The nonlinear optimization routine in Origin is superior to that in Excel. Thus, we report a K_d of 21 ± 2 nM, as definitive in 0.200 M NaCl and the μ = 0.009 M buffer for the sequences shown in Figure 1.

Alternative Counterions. Mg^{2+} ions are known to stabilize double helices more than Na^+, which should disfavor two or more proteins binding to open the helical stem to form nonspecific complexes. Also, divalent ions in the counterion atmosphere screen electrostatic interactions more effectively than monovalent ions. Our results showed that divalent Mg^{2+} ions shift the distribution of species away from $R_1P_{n>1}$ complexes to form exclusively R_1P_1 complexes over the full range of ionic strengths examined for $MgCl_2$ (0.05−0.3 M). We also noted with regard to Figure 6 that addition of 18 mM $MgCl_2$ to the μ = 0.009 M buffer produced the same 1:1 binding affinity as addition of 200 mM NaCl. There are situations, e.g., in NMR spectroscopy, where it is an advantage to use 18 mM $MgCl_2$ in the buffer, and maintain equivalence to the affinity observed for nearly physiological salt concentrations, while disfavoring the formation of $R_1P_{n>1}$ complexes (*43*).

Both acetate and sulfate ions increase the stability of R_1P_1 complexes over chloride, although the destabilization by Mg^{2+} is much stronger in solutions at the same ionic strength. Perhaps OAc^- and SO_4^{2-} are better able to stabilize the protein in its binding conformation compared to Cl^-. Although NC-bound SO_4^{2-} should efficiently screen the ionic attraction between SL3 and NCp7, this destabilizing effect is apparently outweighed by the stabilizing influence that sulfate confers on the protein in the complex.

Stoichiometry. The stoichiometry of the complexes is an important issue. Figure 4 and Figures S1−S4 of the Supporting Information show that $R_1P_{n>1}$ complexes or their mixtures with R_1P_1 can be easily distinguished from 1:1 complexes in the W37 fluorescence-based assays. R_1P_1, R_1P_2, and R_1P_3 complexes have been observed by mass spectrometry (MS) for SL3 in the presence of excess NCp7 (*41*). For the DNA octamer, $[d(TG)]_4$, observations by surface plasmon resonance (SPR) and MS have shown that both D_1P_1 and D_1P_2 complexes form in interactions with NCp7 complexes; the affinity for the second protein is ∼5 times lower than in the formation of the D_1P_1 complex as determined by SPR (*42*).

Diagnosing the presence of complexes with $R_{n>1}P_1$ stoichiometries is problematic using the W37 fluorescence assays, where binding of only the first high-affinity RNA can completely quench the fluorescence. D_2P_1 complexes have been observed by SPR, where the affinity of NCp7 for the second $[d(TG)]_4$ is ∼300 times lower than that for the first; this much lower-affinity D_2P_1 complex was not observed by mass spectrometry (MS) in the same report (*42*). Likewise, $R_{n>1}P_1$ complexes were not observed by MS for SL3−NCp7 complexes (*41*). Therefore, it is likely that excess RNA complexes can be ignored in studies of the sequence-specific interactions of SL3 with NCp7 in 0.2 M NaCl or 18 mM $MgCl_2$, and in the specific packaging of HIV-1 RNA by NC domains of gag and gag-pol precursors.

Effects of Nonideality. Several points of caution are worth noting with regard to effects on the complexes due to the nature and concentrations of salt, protein, and nucleic acid. (i) Deviations from ideal solution characteristics are large for charged molecules. For instance, at ionic strengths of 0.3 M, the mean ionic activity coefficient, $\gamma_\pm$, is near 0.7 for NaCl (*47*), KCl (*48*), and NaOAc (*49*); near 0.5 for $MgCl_2$ (*50*) and Na_2SO_4 (*51*); and near 0.2 for $MgSO_4$ (*49*). The practical significance is that each increment of added salt produces a smaller effect on K_d at higher salt concentrations than at lower concentrations. In plots such as those in Figure 6, this leads to curvature, with a higher slope at low salt concentrations. That is why we used data only at $\mu \leq$ 0.129 M for $MgCl_2$ (dashed line in Figure 6), to find the $MgCl_2$ concentration that produces a K_d equivalent to that in added 0.200 M NaCl. (ii) Effects due to nonideal solutions are most severe for highly charged species, so it should be expected that concentration-based equilibrium constants (as opposed to activity-based equilibria, which regulate the bound and free protein and nucleic acid species) will vary with the concentration of the macromolecules. Nonideality should exert a stronger effect at higher concentrations of protein and nucleic acid. (iii) Experimental techniques for measuring K_d values are often limited to windows in concentration that do not overlap with each other.

NMR concentrations are typically 300−3000 times greater than that used in this work, isothermal titration calorimetry [ITC, 500 times (*45*)], and mass spectrometry [MS, 30−60 times (*41*)]. Effects due to nonideality could make it difficult to compare the results of experiments measured in these widely differing concentration ranges.

Sample Integrity. Perhaps the greatest single caution regarding future work is the importance of positive controls for the integrity of preparations of SL3 and, especially, NCp7 (see Experimental Procedures). The experience in our laboratory is that a stock solution of NCp7 may be frozen and thawed many times but eventually undergoes a rapid collapse in its affinity for SL3. Thus, fluorescence AddNA assays with SL3 in the $\mu = 0.209$ M buffer with NaCl should be repeated each day before any other experiment is performed. NCp7 degradation may be the most common source of K_d values reported in the literature that are substantially higher than the predictions in Figure 6 for $\mu \geq 0.2$ M.

Comparison with Published Analyses of the SL3−NCp7 Interaction. Including their own report, Hagan and Fabris (*41*) collected data from 10 publications on the K_d and stoichiometry of SL3−NC complexes. More recently, $R_1P_{n>1}$ complexes were observed at low NaCl concentrations using electron paramagnetic resonance (EPR), which changed to an R_1P_1 complex at higher salt concentrations (*44*) in concordance with our results reported here. In these 11 studies, the SL3−NC equilibrium was probed by seven methods at four different salt concentrations (see Table 1 of ref *41*). The results differ widely. The leading cause of the variation is the fact that eight studies were conducted at $\mu \leq 0.05$ M, a point at which our work has demonstrated the common occurrence of $R_1P_{n>1}$ complexes and metastable mixtures of $R_1P_{n>1}$ and R_1P_1 complexes. Other causes may include effects due to nonideality or the fact that some measurements may have been compromised by insufficient positive controls in the integrity of NCp7 and SL3. Also, several of the studies were conducted in unbuffered solutions or at pH values outside the buffering range of the salts added to the solutions, e.g., NaOAc at pH 6−8 (the effect of pH on SL3−NC stoichiometry and affinity has not been determined). We have discussed most of this work previously (*27*, *32*) and now consider two studies further (*41*, *45*).

In the first study, intensities of ions derived from SL3, NCp7, and their R_1P_1, R_1P_2, and R_1P_3 complexes were measured using electrospray ionization mass spectrometry (*41*). They reported a K_d of 180 ± 60 nM for the 1:1 complex in 0.15 M NaOAc (pH 7.5; no buffer or details of adjusting pH were specified). The dependence of K_d on NaOAc concentration in Figure 6 of this work can be used to predict that $K_d = 3$ nM in a buffer that is equivalent to the salt conditions described in ref *41*. The authors suggested that quantification by MS is superior to methods that require curve fitting to determine K_d, such as W37 fluorescence assays. On the other hand, there is great confidence in the W37 assays because (i) assays with SL3 and SL3-GGUG in the $\mu = 0.209$ M buffer exhibit nearly 100% quenching of W37, consistent with an almost perfectly linear correlation between the fluorescence intensity and the free protein concentration, and (ii) the known three-dimensional structure provides a clear mechanism for full quenching by stacking W37 on G318 of SL3. The 60-fold difference in K_d cannot be due to curve fitting errors. In fact, the K_d value measured by ESI MS came from curve fitting to a competition experiment with a variant of SL4, which was separately determined to have a K_d of 1300 ± 500 nM (*41*). Examination of Figure 3 of ref *41* shows that the data show only approximate agreement between the measured intensities and the fitted binding isotherm for the SL4 complex. Resorting to a competition assay is necessitated by the relative insensitivity of the method to directly assay high-affinity complexes and their unbound components. Furthermore, it is an open question whether ionization efficiencies are sufficiently constant to accurately sample the equilibrium populations. Nevertheless, the MS work is clearly valuable because of its unequivocal demonstration of the presence of $R_1P_{n\geq 1}$ complexes when $P_t > R_t$ and the insignificance of $R_{n\geq 1}P_1$ complexes in the SL3−NCp7 system.

In the second study, there is a 2500-fold difference in the K_d value of 170 nM measured by ITC (*45*) at $\mu = 0.05$ M and the K_d value of 0.07 nM extrapolated from Figure 6. Although the K_d values of the MS (180 nM) and ITC experiments (170 nM) appear numerically close to each other, the agreement is fortuitous as the solutions differed in ionic strength by a factor of 3. Using the slope of the NaOAc line in Figure 6 shows that these K_d values actually differ from each other by 60-fold when corrected for ionic strength due to the small ions. Work in progress in our laboratory is aimed at reconciling differences between K_d measurements made by ITC, SPR, electrophoretic mobility shifts, and W37 fluorescence.

Implications for Drug Discovery. Beyond an interest in accurately defining K_d and conditions for study of the 1:1 complex, the simple expedient of comparing affinities at 0.2 M NaCl or 18 mM $MgCl_2$ is sufficient to suppress the non-sequence-specific interactions to the point that anti-NC agents can be found to interrupt the specific interactions (*43*, *52*, *53*).

Implications for Packaging Specificity. In vitro measurements of interactions of NC with RNA and DNA show that the interactions with unpaired bases are much stronger than those with paired strands (*35*, *36*, *42*, *54*). Measuring the affinity for SS RNA is complicated because multiple NCp7 moieties can bind sequences that are longer than five or six unpaired nucleotides (*35*, *36*, *42*, *55*). In previous work, we have measured the K_d values of NCp7 for 35 of the 64 GNNN variants of the wild-type GGAG loop on the SL3 RNA stem at 0.2 M NaCl (*32*, *55*). The data can be used to predict that the overall average affinity for these single-stranded loops (K_d) is 2500 nM. Thus, the specific affinity for the GGAG loop is ~100 times greater than the average of these four-base loops. This ratio of specific to nonspecific binding is comparable to those of many other biological interactions, and probably more than sufficient for HIV-1 to package its full-length RNA over nongenomic fragments and nonviral mRNA. This ratio of specific to nonspecific affinity is similar to that of the antibiotic paromomycin, which has ~100-fold higher affinity for the decoding region A-site of rRNA compared to nonspecific binding to competing secondary sites (*56*).

Implications for Chaperone Activity. Rapid rearrangement of protein−nucleic acid complexes is one of the major components of the NC nucleic acid chaperone function (*5*, *11*, *57*). In Results, we report that addition of concentrated NaCl to $R_1P_{n>1}$ complexes at low salt concentrations produced a rapid rearrangement to the R_1P_1 complex even in the presence of excess protein. It is apparent that the collection of free and bound species can rearrange within seconds with respect to changes in the balance of specific and electrostatic interactions. This is supported by NMR observations (*45*), which showed that free and bound SL3 and NCp7 exhibit exchange cross-peaks having a dissociation rate constant of 5 s^{-1}.

Implications for Analysis of Condensed RNA−NCp7 Interactions. Recent analyses of spin-labeled SL3 interacting with NCp7 at low salt concentrations have been shown by EPR to have intriguing properties that should be similar to those of genomic RNA in mature virions (*44*). AddPro titrations similar to those described in Figure S4 of the Supporting Information may be useful in guiding the construction of nearly pure R_1P_2 complexes.

ACKNOWLEDGMENT

We gratefully acknowledge Drs. Andrew Paoletti and Michael Shubsda, who first noticed the unusual characteristics of AddNA assays at low salt concentrations, and Dr. Chris DeCiantis, who performed the earliest AddPro assays.

SUPPORTING INFORMATION AVAILABLE

Four figures describe theoretical AddNA and AddPro assays at a variety of K_d values and experimental titrations at very low NaCl concentrations. This material is available free of charge via the Internet at http://pubs.acs.org.

REFERENCES

1. Linial, M. L., and Miller, A. D. (1990) Retroviral RNA packaging: Sequence requirements and implications. *Curr. Top. Microbiol. Immunol. 157*, 125–152.
2. Wills, J. W., and Craven, R. C. (1991) Form, function, and use of retroviral gag proteins. *AIDS 5*, 639–654.
3. Oertle, S., and Spahr, P. F. (1990) Role of the gag polyprotein precursor in packaging and maturation of Rous sarcoma virus genomic RNA. *J. Virol. 64*, 5757–5763.
4. Damgaard, C. K., Dyhr-Mikkelsen, H., and Kjems, J. (1998) Mapping the RNA binding sites for human immunodeficiency virus type-1 gag and NC proteins within the complete HIV-1 and -2 untranslated leader regions. *Nucleic Acids Res. 26*, 3667–3676.
5. Williams, M. C., Rouzina, I., Wenner, J. R., Gorelick, R. J., Musier-Forsyth, K., and Bloomfield, V. A. (2001) Mechanism for nucleic acid chaperone activity of HIV-1 nucleocapsid protein revealed by single molecule stretching. *Proc. Natl. Acad. Sci. U.S.A. 98*, 6121–6126.
6. Darlix, J. L., Cristofari, G., Rau, M., Pechoux, C., Berthoux, L., and Roques, B. (2000) Nucleocapsid protein of human immunodeficiency virus as a model protein with chaperoning functions and as a target for antiviral drugs. *Adv. Pharmacol. 48*, 345–372.
7. Muriaux, D., De Rocquigny, H., Roques, B. P., and Paoletti, J. (1996) NCp7 activates HIV-1Lai RNA dimerization by converting a transient loop-loop complex into a stable dimer. *J. Biol. Chem. 271*, 33686–33692.
8. Fu, W., Gorelick, R. J., and Rein, A. (1994) Characterization of human immunodeficiency virus type 1 dimeric RNA from wild-type and protease-defective virions. *J. Virol. 68*, 5013–5018.
9. Rist, M. J., and Marino, J. P. (2002) Mechanism of Nucleocapsid Protein Catalyzed Structural Isomerization of the Dimerization Initiation Site of HIV-1. *Biochemistry 41*, 14762–14770.
10. Prats, A. C., Sarih, L., Gabus, C., Litvak, S., Keith, G., and Darlix, J. L. (1988) Small finger protein of avian and murine retroviruses has nucleic acid annealing activity and positions the replication primer tRNA onto genomic RNA. *EMBO J. 7*, 1777–1783.
11. Hargittai, M. R., Gorelick, R. J., Rouzina, I., and Musier-Forsyth, K. (2004) Mechanistic insights into the kinetics of HIV-1 nucleocapsid protein-facilitated tRNA annealing to the primer binding site. *J. Mol. Biol. 337*, 951–968.
12. Druillennec, S., Caneparo, A., de Rocquigny, H., and Roques, B. P. (1999) Evidence of interactions between the nucleocapsid protein NCp7 and the reverse transcriptase of HIV-1. *J. Biol. Chem. 274*, 11283–11288.
13. Lener, D., Tanchou, V., Roques, B. P., Le Grice, S. F., and Darlix, J. L. (1998) Involvement of HIV-I nucleocapsid protein in the recruitment of reverse transcriptase into nucleoprotein complexes formed in vitro. *J. Biol. Chem. 273*, 33781–33786.
14. de Rocquigny, H., Caneparo, A., Delaunay, T., Bischerour, J., Mouscadet, J. F., and Roques, B. P. (2000) Interactions of the C-terminus of viral protein R with nucleic acids are modulated by its N-terminus. *Eur. J. Biochem. 267*, 3654–3660.
15. Berthoux, L., Pechoux, C., and Darlix, J. L. (1999) Multiple effects of an anti-human immunodeficiency virus nucleocapsid inhibitor on virus morphology and replication. *J. Virol. 73*, 10000–10009.
16. Stephen, A. G., Rein, A., Fisher, R. J., and Shoemaker, R. H. (2003) The nucleocapsid protein as a target for novel anti-HIV drugs. *Curr. Drug Discovery,* 33–36 (August issue).
17. Yuan, Y., Kerwood, D. J., Paoletti, A. C., Shubsda, M. F., and Borer, P. N. (2003) Stem of SL1 RNA in HIV-1: Structure and Nucleocapsid Protein Binding for a 1 × 3 Internal Loop. *Biochemistry 42*, 5259–5269.
18. Cruceanu, M., Stephen, A. G., Beuning, P. J., Gorelick, R. J., Fisher, R. J., and Williams, M. C. (2006) Single DNA molecule stretching measures the activity of chemicals that target the HIV-1 nucleocapsid protein. *Anal. Biochem. 358*, 159–170.
19. Vogt, V. M., and Simon, M. N. (1999) Mass determination of Rous sarcoma virus virions by scanning transmission electron microscopy. *J. Virol. 73*, 7050–7055.
20. Coffin, J. M., Hughes, S. H., and Varmus, H. E. (1997) Retroviruses, Cold Spring Harbor Laboratory Press, Plainview, NY.
21. Gelderblom, H. R. (1991) Assembly and morphology of HIV: Potential effect of structure on viral function. *AIDS 5*, 617–637.
22. Clever, J., Sassetti, C., and Parslow, T. G. (1995) RNA secondary structure and binding sites for gag gene products in the 5′ packaging signal of human immunodeficiency virus type 1. *J. Virol. 69*, 2101–2109.
23. Clever, J. L., Eckstein, D. A., and Parslow, T. G. (1999) Genetic dissociation of the encapsidation and reverse transcription functions in the 5′ R region of human immunodeficiency virus type 1. *J. Virol. 73*, 101–109.
24. Clever, J. L., and Parslow, T. G. (1997) Mutant human immunodeficiency virus type 1 genomes with defects in RNA dimerization or encapsidation. *J. Virol. 71*, 3407–3414.
25. McBride, M. S., and Panganiban, A. T. (1996) The human immunodeficiency virus type 1 encapsidation site is a multipartite RNA element composed of functional hairpin structures. *J. Virol. 70*, 2963–2973.
26. McBride, M. S., Schwartz, M. D., and Panganiban, A. T. (1997) Efficient encapsidation of human immunodeficiency virus type 1 vectors and further characterization of cis elements required for encapsidation. *J. Virol. 71*, 4544–4554.
27. Shubsda, M. F., Paoletti, A. C., Hudson, B. S., and Borer, P. N. (2002) Affinities of Packaging Domain Loops in HIV-1 RNA for the Nucleocapsid Protein. *Biochemistry 41*, 5276–5282.
28. Darlix, J. L., Lapadat-Tapolsky, M., de Rocquigny, H., and Roques, B. P. (1995) First glimpses at structure-function relationships of the nucleocapsid protein of retroviruses. *J. Mol. Biol. 254*, 523–537.
29. Hayashi, T., Ueno, Y., and Okamoto, T. (1993) Elucidation of a conserved RNA stem-loop structure in the packaging signal of human immunodeficiency virus type 1. *FEBS Lett. 327*, 213–218.
30. Hayashi, T., Shioda, T., Iwakura, Y., and Shibuta, H. (1992) RNA packaging signal of human immunodeficiency virus type 1. *Virology 188*, 590–599.
31. De Guzman, R. N., Wu, Z. R., Stalling, C. C., Pappalardo, L., Borer, P. N., and Summers, M. F. (1998) Structure of the HIV-1 nucleocapsid protein bound to the SL3 ψ-RNA recognition element. *Science 279*, 384–388.
32. Paoletti, A. C., Shubsda, M. F., Hudson, B. S., and Borer, P. N. (2002) Affinities of the Nucleocapsid Protein for Variants of SL3 RNA in HIV-1. *Biochemistry 41*, 15423–15428.
33. Summers, M. F., Henderson, L. E., Chance, M. R., Bess, J. W., South, T. L., Blake, P. R., Sagi, I., Perez-Alvarado, G., Sowder, R. C. I., Hare, D. R., and Arthur, L. O. (1992) Nucleocapsid zinc fingers detected in retroviruses: EXAFS studies of intact viruses and the solution-state structure of the nucleocapsid protein from HIV-1. *Protein Sci. 1*, 563–574.
34. Cornille, F., Mely, Y., Ficheux, D., Savignol, I., Gerard, D., Darlix, J. L., Fournie-Zaluski, M. C., and Roques, B. P. (1990) Solid phase synthesis of the retroviral nucleocapsid protein NCp10 of Moloney murine leukaemia virus and related "zinc-fingers" in free SH forms. Influence of zinc chelation on structural and biochemical properties. *Int. J. Pept. Protein Res. 36*, 551–558.
35. Vuilleumier, C., Bombarda, E., Morellet, N., Gerard, D., Roques, B. P., and Mely, Y. (1999) Nucleic acid sequence discrimination by the HIV-1 nucleocapsid protein NCp7: A fluorescence study. *Biochemistry 38*, 16816–16825.
36. Fisher, R. J., Rein, A., Fivash, M., Urbaneja, M. A., Casas-Finet, J. R., Medaglia, M., and Henderson, L. E. (1998) Sequence-specific

binding of human immunodeficiency virus type 1 nucleocapsid protein to short oligonucleotides. *J. Virol. 72*, 1902–1909.
37. Shubsda, M. F., Kirk, C. A., Goodisman, J., and Dabrowiak, J. C. (2000) Binding of human immunodeficiency virus type 1 nucleocapsid protein to psi-RNA-SL3. *Biophys. Chem. 87*, 149–165.
38. Maki, A. H., Ozarowski, A., Misra, A., Urbaneja, M. A., and Casas-Finet, J. R. (2001) Phosphorescence and Optically Detected Magnetic Resonance of HIV-1 Nucleocapsid Protein Complexes with Stem-Loop Sequences of the Genomic ψ-Recognition Element. *Biochemistry 40*, 1403–1412.
39. Amarasinghe, G. K., Zhou, J., Miskimon, M., Chancellor, K. J., McDonald, J. A., Matthews, A. G., Miller, R. R., Rouse, M. D., and Summers, M. F. (2001) Stem-loop SL4 of the HIV-1 psi RNA packaging signal exhibits weak affinity for the nucleocapsid protein. structural studies and implications for genome recognition. *J. Mol. Biol. 314*, 961–970.
40. Urbaneja, M. A., Wu, M., Casas-Finet, J. R., and Karpel, R. L. (2002) HIV-1 nucleocapsid protein as a nucleic acid chaperone: Spectroscopic study of its helix-destabilizing properties, structural binding specificity, and annealing activity. *J. Mol. Biol. 318*, 749–764.
41. Hagan, N., and Fabris, D. (2003) Direct mass spectrometric determination of the stoichiometry and binding affinity of the complexes between nucleocapsid protein and RNA stem-loop hairpins of the HIV-1 ψ-recognition element. *Biochemistry 42*, 10736–10745.
42. Fisher, R. J., Fivash, M. J., Stephen, A. G., Hagan, N. A., Shenoy, S. R., Medaglia, M. V., Smith, L. R., Worthy, K. M., Simpson, J. T., Shoemaker, R., McNitt, K. L., Johnson, D. G., Hixson, C. V., Gorelick, R. J., Fabris, D., Henderson, L. E., and Rein, A. (2006) Complex interactions of HIV-1 nucleocapsid protein with oligonucleotides. *Nucleic Acids Res. 34*, 472–484.
43. Yang, L. (2008) NMR analysis of structural features of the HIV-1 nucleocapsid protein in response to mutation and interaction with RNA and drug candidates. Ph.D. Dissertation, Syracuse University, Syracuse, NY.
44. Xi, X., Sun, Y., Karim, C. B., Grigoryants, V. M., and Scholes, C. P. (2008) HIV-1 nucleocapsid protein NCp7 and its RNA stem loop 3 partner: Rotational dynamics of spin-labeled RNA stem loop 3. *Biochemistry 47*, 10099–10110.
45. Amarasinghe, G. K., De Guzman, R. N., Turner, R. B., Chancellor, K. J., Wu, Z. R., and Summers, M. F. (2000) NMR structure of the HIV-1 nucleocapsid protein bound to stem-loop SL2 of the ψ-RNA packaging signal. Implications for genome recognition. *J. Mol. Biol. 301*, 491–511.
46. Cantor, C. R., and Schimmel, P. R. (1980) Biophysical Chemistry, Part III: The behavior of biological macromolecules, W. H. Freeman, San Francisco.
47. Truesdell, A. H. (1968) Activity Coefficients of Aqueous Sodium Chloride from 15 to 50 °C Measured with a Glass Electrode. *Science 161*, 884–886.
48. Hostetler, P. B., Truesdell, A. H., and Christ, C. L. (1967) Activity Coefficients of Aqueous Potassium Chloride Measured with a Potassium-Sensitive Glass Electrode. *Science 155*, 1537–1539.
49. Weast, R. C., and Astle, M. J. (1982) CRC Handbook of Chemistry and Physics, 63rd ed., CRC Press, Boca Raton, FL.
50. Stokes, R. H., and Robinson, R. A. (1948) Ionic hydration and activity in electrolyte solutions. *J. Am. Chem. Soc. 70*, 1870–1878.
51. Robinson, R. A., and Stokes, R. H. (1959) Electrolyte Solutions, Butterworths, London.
52. DeCiantis, C. L., Jensen, D. K., Hudson, B. S., and Borer, P. N. (2007) A nucleic acid switch triggered by the HIV-1 nucleocapsid protein. *Biochemistry 46*, 9164–9173.
53. Deciantis, C. L. (2008) A FRET Based Bistable Oligonucleotide Switch, AlloSwitch, Designed for Specific Recognition of HIV-1 NCp7 and Use in High Throughput Screening. Ph.D. Dissertation, Syracuse University, Syracuse, NY.
54. Wenner, J. R., Williams, M. C., Rouzina, I., and Bloomfield, V. A. (2002) Salt dependence of the elasticity and overstretching transition of single DNA molecules. *Biophys. J. 82*, 3160–3169.
55. Paoletti, A. C. (2004) Affinity of the HIV-1 nucleocapsid protein for structural motifs in the genomic RNA packaging domain. Ph.D. Dissertation, Syracuse University, Syracuse, NY.
56. Kaul, M., Barbieri, C. M., Kerrigan, J. E., and Pilch, D. S. (2003) Coupling of drug protonation to the specific binding of aminoglycosides to the A site of 16 S rRNA: Elucidation of the number of drug amino groups involved and their identities. *J. Mol. Biol. 326*, 1373–1387.
57. Cruceanu, M., Gorelick, R. J., Musier-Forsyth, K., Rouzina, I., and Williams, M. C. (2006) Rapid kinetics of protein-nucleic acid interaction is a major component of HIV-1 nucleocapsid protein's nucleic acid chaperone function. *J. Mol. Biol. 363*, 867–877.